Role of body temperature variations in bats immune response to viral infections

Maria Rita Fumagalli[a,b], Stefano Zapperi[c,d], Caterina A. M. La Porta[a,b]

[a] *Center for Complexity and Biosystems, Department of Environmental Science and Policy, University of Milan, via Celoria 26, 20133 Milano, Italy*
[b] *CNR - Consiglio Nazionale delle Ricerche, Biophysics institute, Genova, Italy*
[c] *Center for Complexity and Biosystems, Department of Physics, University of Milan, via Celoria 16, 20133 Milano, Italy*
[d] *CNR - Consiglio Nazionale delle Ricerche, ICMATE, Via R. Cozzi 53, 20125 Milano, Italy*

Abstract

The ability of bats to coexist with viruses without being harmed is an interesting issue that is still under investigation. Here we use a mathematical model to show that the pattern of body temperature variations observed in bats between day and night is responsible for their ability to keep viruses in check. From the dynamical systems point of view, our model displays an intriguing quasi-periodic behavior that might be relevant in making the system robust by avoiding viral escape due to perturbations in the body temperature cycle.

Keywords:
Bats, IFN-α, Immunity, virus,

1. Background and motivation

Bats provide a natural reservoir for several viruses of clinical importance, including rabies virus, Nipah, Hendra, Ebola and many coronaviridae [1] including SARS-CoV-2 [2]. It is, however, still unclear how bats are able to sustain chronic viral infection without harm. Understanding this issue could have tremendous relevance for the prevention and treatment of viral infections in humans and livestock. Bats are represented by more than 1400 species, about one fourth of all existing mammal species, populating every kind of habitat and being the only mammals capable of sustained flight [3].

Some species of bats are capable of hibernating during the winter season when the temperature decreases, prey are scarce and food requirements can easily exceed available resources [4, 5]. During the day, most bats decrease their activity and enter torpor in order to hunt at dawn when the external temperature is lower and food is more abundant [6, 7]. During flight, the body temperature of bats rises above 40°C [8] while during daily torpor it is significantly lower [6], reaching in some cases 10° C [5]. This is an effective method of energy conservation which is particularly useful to bats since flight has a high energetic cost [8, 5]. Recent work showed that neuronal stimulation is able to induce torpor and decrease the body temperature [9, 10], suggesting that the day/night cycle might not be the only relevant cause of torpor [11].

Here, we show that the variations in bats body temperature are at the core of their unconventional coexistence with viruses. To this end, we construct a mathematical model of the interactions between the virus and the bats immune system. We chose the model parameters so that they match the observed time-dependent body temperature variations and other existing experimental measurements.

2. Bats body temperature variations

The gradient of body temperature (T_b) variations during day/night cycle in bats is estimated as 0.1-0.2° C/min [12, 13, 14] (see Fig.1a, reporting data from [14]). While the range of variation of T_b depends

Email address: caterina.laporta@unimi.it (Caterina A. M. La Porta)

on the species and is correlated to the environmental temperature [14, 15], the absolute value of T_b is affected by the method used to measure it, with differences of $1-2°C$ between internal body and skin temperature. Considering four different datasets on seven species of bats where changes in body or skin temperature was measured on single individuals in both torpid and active states at different environmental temperatures [14, 15], we found that T_b changes roughly between 20-37°C , and $\Delta T_b \approx 10 \pm 4°$ C (Fig.1b). The temperature interval might be even larger, since body temperatures during flight periods could easily reach values as high as 40° C (Fig.1b).

To evaluate the reduction in viral reproduction rate α during the torpid phase, we considered the model proposed by Chen and coworkers [16]. As reported in Fig.1c, under the hypothesis that the virus has its optimal growth rate $\alpha_0 = \alpha_A$ when $T_b = T_{awake}$, we can estimate a reduction of $50-80\%$ of the growth during the torpid phase (α_T). This reduction could also be influenced by other factors, including the elevated presence in bats of heat shock-proteins that could also help control viral growth.

3. Model for viral-host interactions in bats

We developed a minimal model of virus/host interaction in order to evaluate how a reduced viral growth during the torpid phase could contribute to the permanence of chronic viral infection in bats. We investigate Virus-host interactions using a modified Lotka-Volterra predator-prey model with two species representing a single type of virus and the host immune response, which increases in presence of the pathogen and interacts with it by decreasing its diffusion in the organism. We modeled two different kinds of immune responses: the lytic response where the infected cells are destroyed and the nonlytic response where there is an inhibition of viral replication by soluble mediators such as interferons (IFNs) [17].

3.1. Model description

Following [17], we describe virus/host interactions as

$$\begin{cases} \dfrac{dv(t)}{dt} = \dfrac{\alpha(t)}{1+\lambda\, I(t)}\, v(t) - \beta\, v(t) I(t) - \mu\, v(t) \\ \dfrac{dI(t)}{dt} = \gamma\, v(t) - \delta\, I(t) \end{cases} \tag{1}$$

where v and I represent virus load and immune response strength, μ and δ are the virion and immune response half-lives and $\alpha(t)$ is the virus growth rate as a function of time. In virus-host interaction models for specific viruses (i.e. HIV), the population of susceptible and infected cells are usually included, since the exhaustion of the healthy cells reservoir is an important feature of the infection dynamics. Here, we aim to model virus-host interactions in bats considering viruses that do not target specific cell types. Thus, we do not explicitly model susceptible and infected cells but consider an infinite reservoir of healthy host cells. Similarly, we do not include in the model the source of the immune response. Hence I does not represent a specific cell type or mediator but only the intensity of the response.

The parameter λ is related to the effect of the nonlytic immune response, that decreases virus reproduction, while β is an effective contribution to virus degradation due to the lytic process. We study the nonlytic ($\lambda > 0$, $\beta = 0$) and the lytic ($\lambda = 0$, $\beta > 0$) responses separately. The induction of an immune response is controlled by the parameter γ and does not depend on the actual value of I. This assumption is coherent with the known mechanism of production of IFN-α, that is not auto-activated but released from infected cells. In principle, immune response induction should be limited (i.e. $\propto v(t)/(v(t)+\nu)$), implying a limited growth of I when $v(t) >> \nu$. Here, we focus on chronic, controlled virus infection where the immune response is far from saturation and thus, in our model, the immune system is capable of contrasting the virus producing a (virtually) infinite response.

In both lytic and nonlytic systems, the first equilibrium point is a saddle point corresponding to the extinction of both species $(I_{eq}, v_{eq}) = (0, 0)$. The second equilibrium point for the lytic case is given by

$$(I_{eq}, v_{eq}) = \left(\frac{\alpha(t) - \mu}{\beta}, \frac{\delta(\alpha(t) - \mu)}{\gamma} \right) \tag{2}$$

and is stable for $\delta > 4(\alpha(t) - \mu)$ and a stable spiral otherwise.

In the nonlytic case, the second equilibrium point is instead given by

$$(I_{eq}, v_{eq}) = \left(\frac{\alpha(t) - \mu}{\mu\lambda}, \frac{\delta(\alpha(t) - \mu)}{\mu\gamma} \right) \tag{3}$$

and is stable for $\alpha(t) > \mu$.

3.2. Model parameters

The half-life of IFNα is estimated to be $\approx 4 - 5$h, even if shorter lifetimes have been observed [18] and free virions half-life in serum are in the same range for HIV, HCV and Influenza-A virus [19]. Thus, we assume $\delta \approx \mu \approx \ln(2)/4 \approx 0.15$. If we identify the parameter δ with the decay rate of the IFN-induced response genes (i.e. the decrease of the effective action of the immune response) $\delta \approx \ln(2)/8\text{h} \approx 0.9\text{h}^{-1}$ is of the same order of magnitude [20]. The viral growth rate is given by the product between the burst size (how many virions are produced) and the first exit time. The burst size varies in the range $10^2 - 10^4$ for different kinds of viruses, while the first exit time can be estimated to be $\approx 6 - 12$h [21, 22]. Considering the upper range of these values (i.e. aggressive, fast viruses), α can be estimated as $\ln(10^4)/6\text{h} \approx 1.5\text{h}^{-1}$. Values of β,λ and γ are more difficult to estimate. A fit of the dose-response curve to IFN-α for different viruses [23, 20] shows that they vary in a wide range of values (i.e. $10 - 10^3$). We verified our results for parameters in the $0.01 - 100$ range, noticing that the relative reduction of v and I are not influenced by the specific value chosen.

4. Model solutions

When the model parameters are not time-dependent, we expect that the model reaches a stable equilibrium point in both lytic and nonlytic conditions. As previously discussed, however, the viral growth rate is expected to change in time ($\alpha(t)$) as a consequence of changes in the host temperature during daily torpor. For the sake of simplicity and due to the experimentally observed sharp transition of T_b, we consider changes in $\alpha(t)$ between α_A and α_T to be instantaneous. We verified that considering a smoother transition of $\alpha(t)$ and including a realistic change of decay rates with temperature δ and μ, the results are not affected. Fig. 1d-f illustrates how a sharp change in $\alpha(t)$ during the day could influence the level of both the virus load and the immune response in bats, leading to a pseudo-periodic behavior. For a wide range of biological parameters, the lytic model effectively displays a stable spiral attractor for both the torpid and the awake phase. As a consequence of this, its associated trajectory spans a larger range of values (see Fig. 1e) while the presence of fixed points leads to more localized trajectories (see Fig. 1f). For both models, a quasi-periodic behavior is reached after a short transient phase.

Fig. 1d shows the presence of daily oscillations with an effective quasi-period of 48h, with transition points that do not coincide exactly from one cycle to the next. To investigate if the observed dynamical behavior is chaotic, we estimate the associated Lyaupnov exponents $\Lambda_\pm$ showing that the maximum exponent Λ_+ can become transiently positive for a specific range of parameters (either $\gamma_{\text{lytic}} \gg 1$ or $\beta \gg 1$) but does not display true long-term chaotic behavior (Fig.2a). The existence of pesudo-periodic behavior with a period larger than 24h depends on the duration of torpid and awake states (i.e. on t_{night}) and on the ratio α_S/α_T. Fig. 2b shows the amount of time spent, each day, below the equilibrium values of the wake state over a period of 10 days. It is evident that for intermediate durations of the awake phase, more than one value is possible, corresponding to 2-day or 4-days periods, as in Fig.1c. The nonlytic

model shows a less variable behavior, and for longer time scales ($\approx 100d$) the system becomes effectively periodic with period $24h$ for any duration of t_{night} and α. We verified that Λ_+ is transiently positive also in presence of noise in t_{night} or in t_{day}. In particular, we tested the results with $t_{\text{night}} = 8\text{h} \pm \Delta t$, where Δt is uniformly distributed between $[-\Delta_0, 1Delta_0]$ and $\Delta_0 = 1, 2, 4\text{h}$, and with similar fluctuations for t_{day}. Under these conditions, the quasi-periodic behavior observed in the absence of noise is still preserved.

Since we are interested in long-term effects, we evaluate the amount of both v and I averaged over ten days (i.e. more than one period). Interestingly, the average amount of virus and immune response load are very similar for both models, indicating a pronounced reduction compared to equilibrium values even at larger t_{night} and for minimal changes in α (see Fig. 2c). Evaluating the amount of time spent by the system in the region $v < v_{\text{awake}}$ and $I < I_{\text{awake}}$ shows that the nonlytic model is capable of maintaining a more stable viral reduction (Fig. 2d) while a more complex picture, corresponding to the existence of two-days period is shown by the lytic model (Fig.2e,f). Furthermore, the results highlight the different nature of lytic model trajectories, that allows the system to stay in the phase space region where $v > v_{\text{awake}}$ and $I > I_{\text{awake}}$. Note that the model parameters estimated from biological data to describe effective virus-host interactions (β,γ and λ), affect the location of the stable point and the global velocity of the system, but do not affect the values reported in Fig. 2 that are all relative to the equilibrium point. Thus, these results could in principle apply to a wide variety of viruses with different strength and efficiency of the immune response.

5. Conclusion

Using a minimal model of virus-host interactions, we were able to evaluate the contribution of daily torpor in the maintenance of viral infections in bats. The model is clearly simplified since it does not consider how the virus spreads in the body nor the details of the immune cells. Despite this, the model shows that even with short torpor periods, corresponding to a small virus growth rate reduction, bats are able to achieve a significant reduction of the virus concentration. A comparison of two different models of the immune response shows that the nonlytic response, that is typical of innate immunity triggered by IFN-α, is more efficient in maintaining constantly low viral levels. Furthermore, the presence of daily torpor contributes to a reduction of the immune response, preventing the risks correlated to a sustained inflammation. Recent work demonstrates that virus replication could increase with temperature, without affecting T_b [24, 25]. This could suggest that viral load is limited by torpor, rather than by temperature variations, in contrast with the 'flight as fever' hypothesis [26].

From the dynamical systems point of view, at biologically relevant time scales, both models show intriguing quasi-periodic but non-chaotic behavior. It is possible that the observed quasi-periodic behavior would make the system more robust to noise, such as the one coming from variations in the sleep-wake periodicity.

Author Contributions

MRF solved the model, analyzed data. CAMLP and SZ designed and coordinated the study. CAMLP,MRF and SZ wrote the paper.

Acknowledgements

SZ and CAMLP thank for hospitality the chair of Biological Physics at LMU Munich where this work was completed.

Data Accessibility

The code used to generate all the results in the present paper is available at `https://github.com/ComplexityBiosystems/bats-virus/`.

Funding Statement

No funding for this work.

References

[1] Chen L, Liu B, Yang J, Jin Q. 2014 DBatVir: the database of bat-associated viruses. *Database* **2014**. bau021.

[2] Wacharapluesadee S, Tan CW, Maneeorn P, Duengkae P, Zhu F, Joyjinda Y, Kaewpom T, Chia WN, Ampoot W, Lim BL, Worachotsueptrakun K, Chen VCW, Sirichan N, Ruchisrisarod C, Rodpan A, Noradechanon K, Phaichana T, Jantarat N, Thongnumchaima B, Tu C, Crameri G, Stokes MM, Hemachudha T, Wang LF. 2021 Evidence for SARS-CoV-2 related coronaviruses circulating in bats and pangolins in Southeast Asia. *Nat Commun* **12**, 972.

[3] Jones KE, Bininda-Emonds ORP, Gittleman JL. 2005 Bats, clocks, and rocks: diversification patterns in Chiroptera. *Evolution* **59**, 2243–2255.

[4] Geiser F, Körtner G. 2010 Hibernation and daily torpor in Australian mammals. *Zoologist* **35**, 2.

[5] Geiser F, Stawski C. 2011 Hibernation and Torpor in Tropical and Subtropical Bats in Relation to Energetics, Extinctions, and the Evolution of Endothermy. *Integrative and Comparative Biology* **51**, 337–348.

[6] Ruf T, Geiser F. 2015 Daily torpor and hibernation in birds and mammals. *Biological Reviews* **90**, 891–926.

[7] Stawski C, Willis C, Geiser F. 2014 The importance of temporal heterothermy in bats. *Journal of Zoology* **292**, 86–100.

[8] Thomas SP, Suthers RA. 1972 The Physiology and Energetics of Bat Flight. *Journal of Experimental Biology* **57**, 317–335.

[9] Takahashi T, Sunagawa G, Soya S, Abe M, Sakurai K, Ishikawa K, Yanagisawa M, Hama H, Hasegawa E, Miyawaki A, Sakimura K, Takahashi M, Sakurai T. 2020 A discrete neuronal circuit induces a hibernation-like state in rodents. *Nature* **583**, 109–114.

[10] Hrvatin S, Sun S, Wilcox O, Yao H, Lavin-Peter A, Cicconet M, Assad E, Palmer M, Aronson S, Banks A, Griffith E, Greenberg M. 2020 Neurons that regulate mouse torpor. *Nature* **583**, 1–7.

[11] Rintoul J, Brigham R. 2014 The influence of reproductive condition and concurrent environmental factors on torpor and foraging patterns in female big brown bats (Eptesicus fuscus). *Journal of comparative physiology. B, Biochemical, systemic, and environmental physiology* **184**, 777–787.

[12] Kelm DH, von Helversen O. 2007 How to budget metabolic energy: torpor in a small Neotropical mammal. *Journal of Comparative Physiology B* **177**, 667–677.

[13] Coburn DK, Geiser F. 1998 Seasonal changes in energetics and torpor patterns in the subtropical blossom-bat Syconycteris australis (Megachiroptera). *Oecologia* **113**, 467–473.

[14] Bartels W, Law B, Geiser F. 1998 Daily torpor and energetics in a tropical mammal, the northern blossom-bat Macroglossus minimus (Megachiroptera). *Journal of comparative physiology. B, Biochemical, systemic, and environmental physiology* **168**, 233–9.

[15] Wojciechowski M, Jefimow M, Tegowska E. 2007 Environmental conditions, rather than season, determine torpor use and temperature selection in large mouse-eared bats (Myotis myotis). *Comparative biochemistry and physiology. Part A, Molecular & integrative physiology* **147**, 828–40.

[16] Chen P, Shakhnovich E. 2010 Thermal Adaptation of Viruses and Bacteria. *Biophysical journal* **98**, 1109–18.

[17] Wodarz D, Christensen JP, Thomsen AR. 2002 The importance of lytic and nonlytic immune responses in viral infections. *Trends in Immunology* **23**, 194–200.

[18] Shechter Y, Preciado-Patt L, Schreiber G, Fridkin M. 2001 Prolonging the half-life of human interferon-alpha 2 in circulation: Design, preparation, and analysis of (2-sulfo-9-fluorenylmethoxycarbonyl)7- interferon-alpha 2. *Proceedings of the National Academy of Sciences* **98**, 1212–1217.

[19] Perelson A. 2002 Modelling Viral and Immune System Dynamics. *Nature reviews. Immunology* **2**, 28–36.

[20] De La Cruz-Rivera PC, Kanchwala M, Liang H, Kumar A, Wang LF, Xing C, Schoggins JW. 2018 The IFN Response in Bats Displays Distinctive IFN-Stimulated Gene Expression Kinetics with Atypical RNASEL Induction. *The Journal of Immunology* **200**, 209–217.

[21] Sanjuán R, Nebot MR, Chirico N, Mansky LM, Belshaw R. 2010 Viral Mutation Rates. *Journal of Virology* **84**, 9733–9748.

[22] Baccam P, Beauchemin C, Macken CA, Hayden FG, Perelson AS. 2006 Kinetics of Influenza A Virus Infection in Humans. *Journal of Virology* **80**, 7590–7599.

[23] da Rocha Matos A, Wunderlich K, Schloer S, Schughart K, Geffers R, Seders M, de Witt M, Christersson A, Wiewrodt R, Wiebe K, Barth P, Hocke A, Hippenstiel S, Hönzke K, Dittmer U, Sutter K, Rescher U, Rodionycheva S, Matera N, Ludwig S, Brunotte L. 2019 Antiviral potential of human IFN-a subtypes against influenza A H3N2 infection in human lung explants reveals subtype-specific activities. *Emerging Microbes & Infections* **8**, 1763–1776. PMID: 31826721.

[24] Munster V, Adney D, van Doremalen N, Brown V, Miazgowicz K, Milne-Price S, Bushmaker T, Rosenke R, Scott D, Hawkinson A, Wit E, Schountz T, Bowen R. 2016 Replication and shedding of MERS-CoV in Jamaican fruit bats (Artibeus jamaicensis). *Scientific Reports* **6**, 21878.

[25] Miller M, Mcminn R, Misra V, Schountz T, Müller M, Kurth A, Munster V. 2016 Broad and Temperature Independent Replication Potential of Filoviruses on Cells Derived From Old and New World Bat Species. *Journal of Infectious Diseases* **214**, jiw199.

[26] O'Shea T, Cryan P, Cunningham A, Fooks A, Hayman D, Luis A, Peel A, Plowright R, Wood J. 2014 Bat Flight and Zoonotic Viruses. *Emerging infectious diseases* **20**, 741–5.

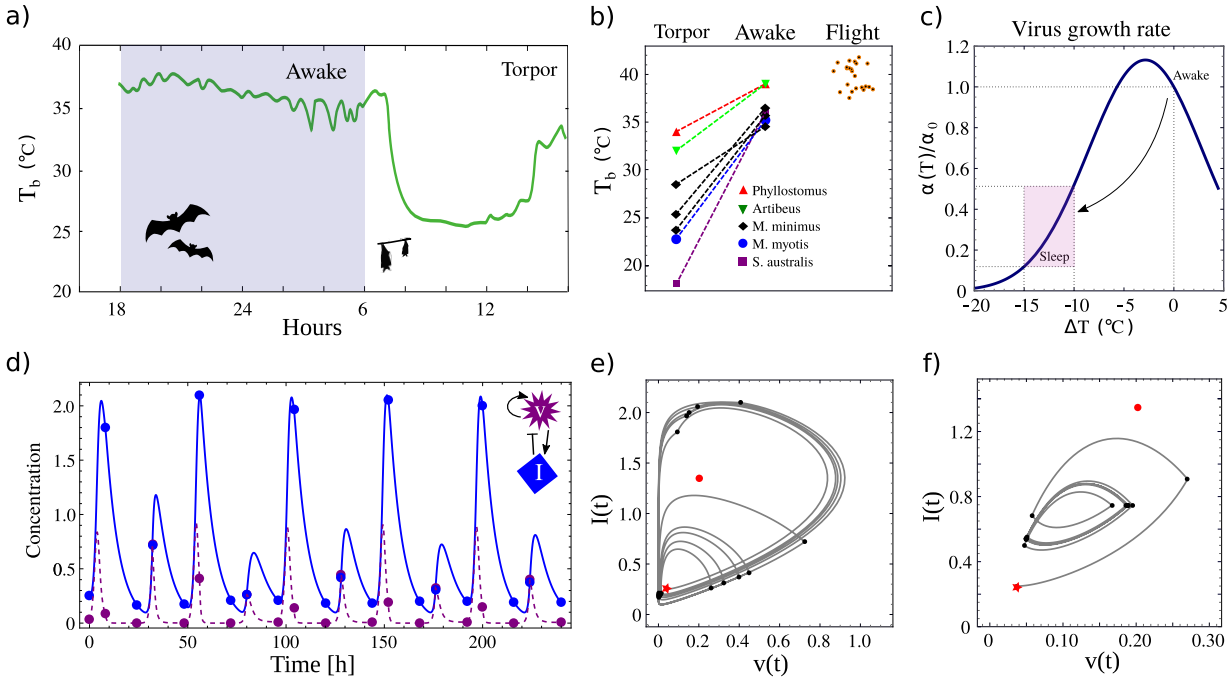

Figure 1: a) Representative illustration of T_b for a bat during night (shaded area) and its drastic reduction when entering torpor during the day. Data from [14]. b)Change of temperature between torpid and awake phase for five different species or genera of bats, as in legend. Average temperature of 21 bats species are also reported (orange dots) [26]. c) Thermal response curve of viral growth rate. Shaded region corresponds to typical range of ΔT for bats during daily torpor. Curve is obtained as in Ref.[16]. d-f) Typical trajectory from the numerical solutions of lytic (d,e) and nonlytic models (f) including day/night cycle. Starting point is stable point corresponding to day parameters (torpor condition, red star in Panels (e,f). When bats awake, virus growth rate increases and the system moves toward the new equilibrium point ($(v_{\rm awake}, I_{\rm awake})$, red dots in Panels (e,f). After a given time (t_{night}), parameters are reverted to diurnal values for a time $t_{\rm day} = 24 - t_{\rm night}$ and the system tend to return to torpor stable state. Blue/purple dots in Panel (d) and black dots in Panels (e,f) indicate transition point between night/day when virus growth rate is switched on/off. For both the models $t_{\rm night} = 8$,$\alpha_A = 1.5$,$\alpha_T = 0.4$,$\delta = 0.15$, $\mu = 0.15$; β, γ, λ are chosen to have the same equilibrium points for the two models: $\beta = \gamma = 1$, $\lambda = 6.67$,$\gamma = 0.15$.

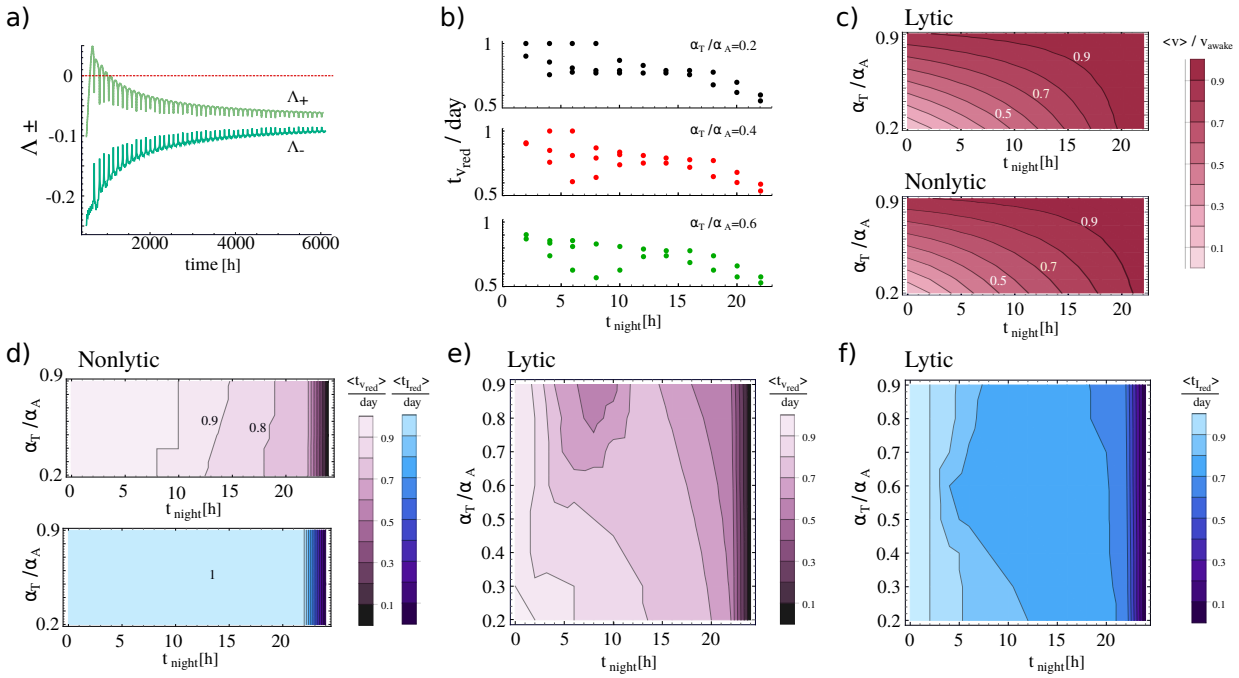

Figure 2: a) An example of transiently positive Lyaupnov exponent calculated for the lytic model. Light and dark green lines represent the two Lyaupnov exponents. Parameters are set as follows: $t_{\text{night}} = 8h$, $\alpha_A = 1.5$,$\alpha_T = 0.4$,$\delta = 0.15$, $\mu = 0.15$, $\beta = 1$, $\gamma = 50$. b) For lytic model, we evaluated the fraction of time that is spent by the system in the region $v < v_{\text{awake}}$ ($t_{v_{\text{red}}}$) each day over 10 days period for different values of t_{night}. The existence of 2-3 points for the same duration of awake phase indicates the period of the system is longer than $24h$ and thus reduction varies between one day and the next one. c) Average value of v was calculated over 10 days for both lytic and nonlytic models and the ratio between $< v >$ and v_{awake} is reported for different values of the parameters. d-f) Average fraction of time that is spent by the system in the region $v < v_{\text{awake}}$ and $I < I_{\text{awake}}$ id reported for nonlytic (d) and lytic (e,f) models. The initial condition of the system is always set to torpid equilibrium point. We considered data from day 50 onward, to avoid transient adaptation phase. Parameters as follows: $\alpha_A = 1.5$,$\delta = 0.15$, $\mu = 0.15$,$\beta = 1$, $\lambda = 6.67$,$\gamma = 0.15$.